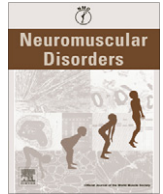




Contents lists available at ScienceDirect

Neuromuscular Disorders

journal homepage: www.elsevier.com/locate/nmd

Dystrophin-deficient zebrafish feature aspects of the Duchenne muscular dystrophy pathology

Joachim Berger^a, Silke Berger^a, Thomas E. Hall^a, Graham J. Lieschke^b, Peter D. Currie^{a,*}

^aAustralian Regenerative Medicine Institute, Monash University, Clayton Campus, VIC 3800, Australia

^bCancer and Haematology Division, Walter and Eliza Hall Institute of Medical Research, Parkville, VIC 3052, Australia

ARTICLE INFO

Article history:

Received 7 May 2010

Received in revised form 12 July 2010

Accepted 17 August 2010

Available online xxx

Keywords:

Dystrophin

DMD

Duchenne muscular dystrophy

Zebrafish

Muscle

ABSTRACT

Duchenne muscular dystrophy is caused by mutations in the dystrophin gene. As in humans, zebrafish dystrophin is initially expressed at the peripheral ends of the myofibres adjacent to the myotendinous junction and gradually shifts to non-junctional sites. Dystrophin-deficient zebrafish larvae are characterised by abundant necrotic fibres being replaced by mono-nucleated infiltrates, extensive fibrosis accompanied by inflammation, and a broader variation in muscle fibre cross-sectional areas. Muscle progenitor proliferation cannot compensate for the extensive skeletal muscle loss. Live imaging of dystrophin-deficient zebrafish larvae documents detaching myofibres elicited by muscle contraction. Correspondingly, the progressive phenotype of dystrophin-deficient zebrafish resembles many aspects of the human disease, suggesting that specific advantages of the zebrafish model system, such as the ability to undertake *in vivo* drug screens and real time analysis of muscle fibre loss, could be used to make novel insights relevant to understanding and treating the pathological basis of dystrophin-deficient muscular dystrophy.

© 2010 Elsevier B.V. All rights reserved.

1. Introduction

Duchenne muscular dystrophy (DMD) is a progressive muscle wasting disorder, which results from mutations within the dystrophin gene. Loss of dystrophin function results in cycles of skeletal muscle fibre degeneration and regeneration during which the capacity for skeletal muscle regeneration is progressively exhausted, leading to loss of muscle function and death in late teen to early thirties. In skeletal muscle, dystrophin provides a link between the actin cytoskeleton and the extracellular matrix, which has led to the hypothesis that muscle breakdown in DMD patients is caused, at least in part, by the lack of a stable link between the extracellular matrix and the dystrophic muscle cell, resulting in damage to the sarcolemmal membrane and consequent fibre loss [1]. Another hypothesis is based on dystrophin serving as a scaffold protein for the assembly of the dystrophin–glycoprotein complex, as disruption of this multi-component complex impairs sarcolemmal membrane integrity resulting in increased influx of Ca^{2+} [2].

Despite the inevitably fatal nature of DMD, no effective therapy has yet been developed. While the current animal models of DMD have generated valuable insights to the pathological basis of the disease and have been instrumental to the development of therapeutic approaches each has their limitation. The most commonly used model, the *mdx* mouse [3], lacks many aspects of the human

DMD pathology [4,5], but does possess the ability to be genetically manipulated with relative ease. Other mammalian model systems, such as the dystrophin-deficient dog does reflect the human condition more closely, but have other disadvantages like phenotypic variability [6], difficult statistical elaboration of phenotypes, and limited genetic tractability that make them less valuable for evaluating therapeutic strategies. Thus, an animal model that possess a highly penetrant dystrophic phenotype, relevant to the human condition, that could also easily be genetically manipulated would be a valuable adjunct to existing dystrophic models.

Zebrafish models of disease are particularly valuable because their embryos develop *ex utero*, are translucent, highly manipulable, and genetically tractable [7]. In a large-scale zebrafish screen, the *dmd*^{ta222a} mutant (synonyms: *sapje*, *sap*) was isolated [8] and identified by us as a carrier of a null mutation in the orthologous dystrophin gene [9]. In homozygous *dmd*^{ta222a/ta222a} embryos, dystrophin is lost at the myotendinous junction causing muscle detachment as detected by a reduction in birefringency [9]. However, this study did not examine the role of dystrophin at the non-junctional sarcolemma in zebrafish, failure of which is thought to underlie much of the damage incurred in human DMD sufferers [10]. We therefore sought to fully characterise the dystrophin expression throughout the development of muscle fibres in zebrafish and to fully characterise the pathology evident in larval stages of dystrophin-deficient zebrafish until their death at 31 days post fertilization (dpf), as these might be more relevant to the human disease.

* Corresponding author. Tel.: +61 3 99029602; fax: +61 3 99029729.

E-mail address: Peter.Currie@ARMI.Monash.edu.au (P.D. Currie).

Histological characterisation of homozygous *dmd*^{ta222a/ta222a} larvae show that extensive muscle degeneration is accompanied by fibrosis, inflammatory response, activation of the muscle stem cell compartment, and greater variation in myofibre cross-sectional areas (CSA). Surveyed pathologies resemble the progressive human condition suggesting that dystrophin-deficient zebrafish may accurately model aspects of the human condition. In addition, live imaging of translucent *dmd*^{ta222a/ta222a} mutant larvae indicates that myofibre snapping is triggered upon muscle contraction. This study further suggests that the zebrafish model may be a useful tool to evaluate therapies early in their development and provide a relevant model in which to undertake high-throughput drug discovery approaches that are currently being deployed in zebrafish [11].

2. Materials and methods

2.1. Zebrafish lines and maintenance

The *dmd*^{tm90c} and *dmd*^{ta222a} mutant alleles were obtained from the Tübingen Stock Collection [8]. Animal experiments were approved by MAS/2009/05.

2.2. Immunohistochemistry and muscle morphometry

Cryostat cross sections were stained with Harris Hematoxylin and Eosin (H&E), by using the Azan–Mallory technique, or immunostained as described [12]. Mouse monoclonal antibodies used were: Pax7 (DSHB), dystrophin (Mandra1, DSHB), and BrdU (Roche). BrdU labelling was performed by soaking larvae in 1% BrdU solved in fish water. 7 *dmd*^{ta222a/ta222a} homozygous and 7 siblings were utilised for determining the BrdU labelling index of 7 dpf old fish. For the other stages (14, 21, and 28 dpf) 4 independently bred fish of each genotype and stage were used. Labelling of the sarcolemma was performed with rhodamine conjugated wheat germ agglutinin as described (1:100, Vector Laboratories) [13]. Electron micrographs were taken with a Philips (Eindhoven, The Netherlands) EM410 transmission electron microscope.

2.3. Morphometric analysis

Cryofrozen sections were H&E stained and fibre CSA measured. Fibres of the whole epaxial myotome were measured for CSA by using Image 1.63 software (Scion Corporation, Frederick, MD). For each genotype the following amount of sections were measured: $n=4$ for 7 dpf, $n=3$ for 14 and 21 dpf, and $n=2$ for 28 dpf. The CSA of muscle fibres smaller than $60 \mu\text{m}^2$ were expressed as percentage of the total number of epaxial muscle fibres. The CSA of large muscle fibres were expressed as percentage of the total area covered by epaxial muscle fibres. Data are shown as mean \pm SEM with significance determined by Student's *t*-test.

2.4. Time-lapse photomicroscopy

Fish larvae (3 dpf) were anaesthetized with the broad voltage-gated sodium channel blocker tricaine, embedded into 1% agarose, and orientated to give a lateral view of the trunk muscle. Subsequent myofibre behavior of embedded larvae was observed under differential interference contrast (DIC) light conditions. After a 10 min time gap, the anaesthetic was removed by exchange of the immersion media. The time course of 10 min during the anaesthetic stage and 10 min after anaesthetic removal was monitored using a Zeiss AxioCam MRm digital camera.

3. Results

3.1. Histological characterization of the myopathy in *dmd*^{ta222a}

In the human embryo, dystrophin is initially expressed predominantly at the peripheral ends of the myofibres, immediately adjacent to the tendons, and gradually shifts to non-junctional sites in the foetal stage [14,15]. It is believed that the structural failure of the non-specialised sarcolemma underlies the majority of aspects of the human disorder. This expression is paralleled by the localisation of zebrafish dystrophin, which in the embryo is expressed exclusively at the peripheral ends of the myofibres or myotendinous junction (Fig. 1A). At 7 dpf dystrophin expression shifts to a more widespread sarcolemmal expression [16,17] that appears initially uneven in its non-junctional sarcolemma distribution, but becomes more robustly expressed and more uniform in its localisation with progressing larval age (Fig. 1B–F).

To characterize the muscle of *dmd*^{ta222a/ta222a} homozygote larvae at similar stages, Hematoxylin and Eosin (H&E) staining was performed on cross sections collected from 7, 14, 21, and 28 dpf old larvae. Throughout the development of homozygous *dmd*^{ta222a/ta222a}, a number of pathological abnormalities were identified that were invariably exacerbated with growing age. There was excessive atrophy with loss of normal muscle fibres, increased variation in fibre size, and degeneration of some myofibres (Fig. 2). Eosinophilic hypercontracted myofibres, one of the earliest signs of dystrophic muscles in human patients [18], are also detected frequently throughout all stages of dystrophin-deficient zebrafish larvae. Also abundant infiltrates of small mono-nucleated cells were associated with the homozygous *dmd*^{ta222a/ta222a} muscle throughout larvae development. We next surveyed the muscle characteristics in more detail.

3.2. Distribution of fibre cross-sectional areas (CSA) of the *dmd*^{ta222a} skeletal trunk muscle

A common pathological hallmark of DMD is the marked broadening of the distribution of CSA of myofibres, due to numerous small regenerating myofibres and some hypertrophic fibres that probably compensate for fibre breakdown [19]. To analyse the fibre CSA of homozygous *dmd*^{ta222a/ta222a} larvae and their siblings, cross sections were stained with H&E and the CSA of all epaxial myofibres were measured. Morphometric analysis of myofibre CSA at 7, 14, 21, and 28 dpf demonstrates that in homozygous *dmd*^{ta222a/ta222a} larvae the proportion of small myofibres (defined as myofibres with a CSA below $60 \mu\text{m}^2$) is significantly higher in comparison to their siblings (Fig. 3A). Also, the area covered by large myofibres (defined as myofibres with a CSA over $400 \mu\text{m}^2$ for 7, $800 \mu\text{m}^2$ for 14, and $1000 \mu\text{m}^2$ for 21 and 28 dpf) is significantly greater in homozygous *dmd*^{ta222a/ta222a} larvae than in their siblings (Fig. 3B). It should also be noted that in homozygous *dmd*^{ta222a/ta222a} larvae the tendency to large fibres is increasing with progressing age with some fibres having a CSA of up to $9000 \mu\text{m}^2$ at 28 dpf (Fig. 3D').

To examine if central nucleation is a feature of the regenerative response in zebrafish dystrophy, we labelled nuclei with Hoechst and used the lectin agglutinin of wheat germ to stain the extracellular matrix associated with the muscle sarcolemma along with connective tissue and blood vessels (Fig. 3C–C'). Trunk muscle fibres with centralised nuclei were identified and calculated as a percentage of total amount of fibres. The percentage of muscle fibres with central nucleation is significantly reduced in homozygous *dmd*^{ta222a/ta222a} larvae compared to their siblings by 0.76 ± 0.06 , 0.27 ± 0.03 , and 0.16 ± 0.03 -fold at 7, 14, and 21 dpf, respectively (data are means \pm SEM). At 28 dpf, a reduction (by

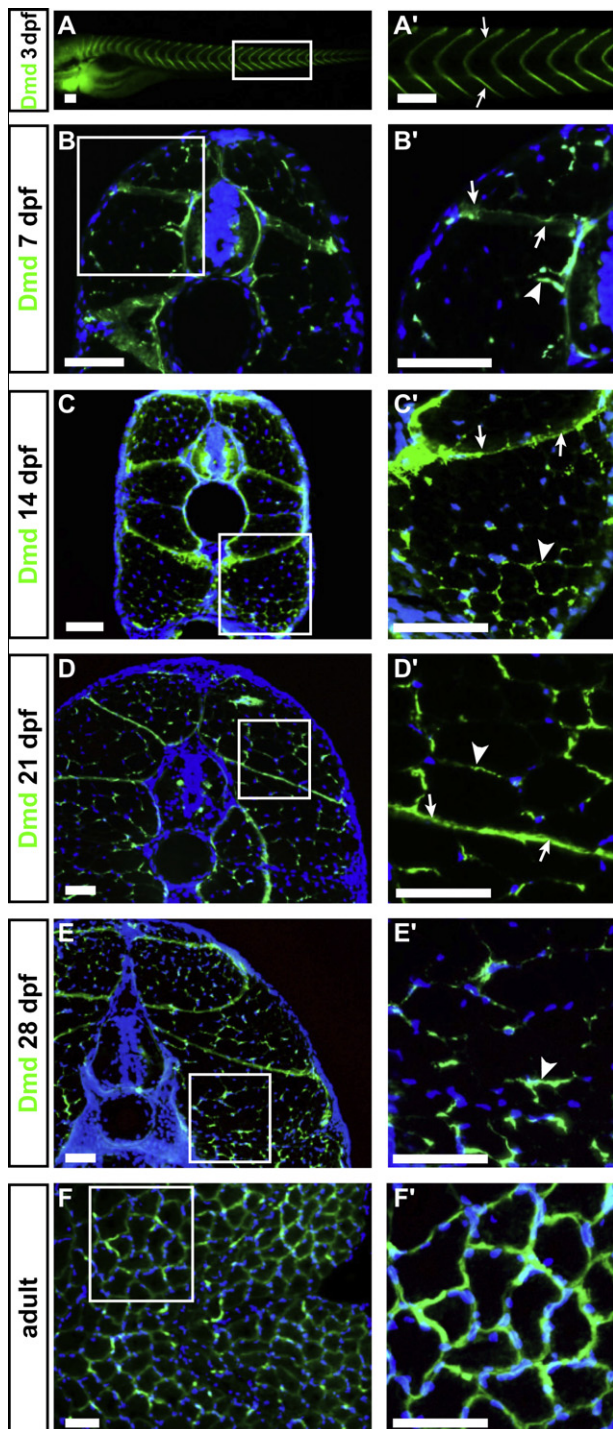


Fig. 1. Ontogeny of dystrophin expression in junctional and non-junctional sarcolemma. Myofibre of 3 days post fertilization (dpf) old wildtype larvae shows dystrophin (DMD) expression, marked in green, only at the myotendinous junction (arrows A'). Expression of dystrophin also becomes localised to the non-junctional sarcolemma from 7 dpf and increases in levels with increasing age, exhibiting robust levels of non-junctional sarcolemmal expression in the adult (B–F). 7 dpf (B and B'); 14 dpf (C and C'); 21 dpf (D and D'); 28 dpf (E and E'); adult stage (F and F'). Magnifications of boxes in A–F (A'–F'). Counter-staining of sections with Hoechst marks nuclei in blue. Scale bar: 50 μ m. Arrows mark expression of dystrophin at the myotendinous junction and arrowheads mark the expression at the non-junctional sarcolemma.

0.6 \pm 0.2) was still detected, but not significant ($P = 0.1$). This unexpected reduction in central nucleation, discussed more fully below, likely reflects a difference in timing of maturation of muscle cells

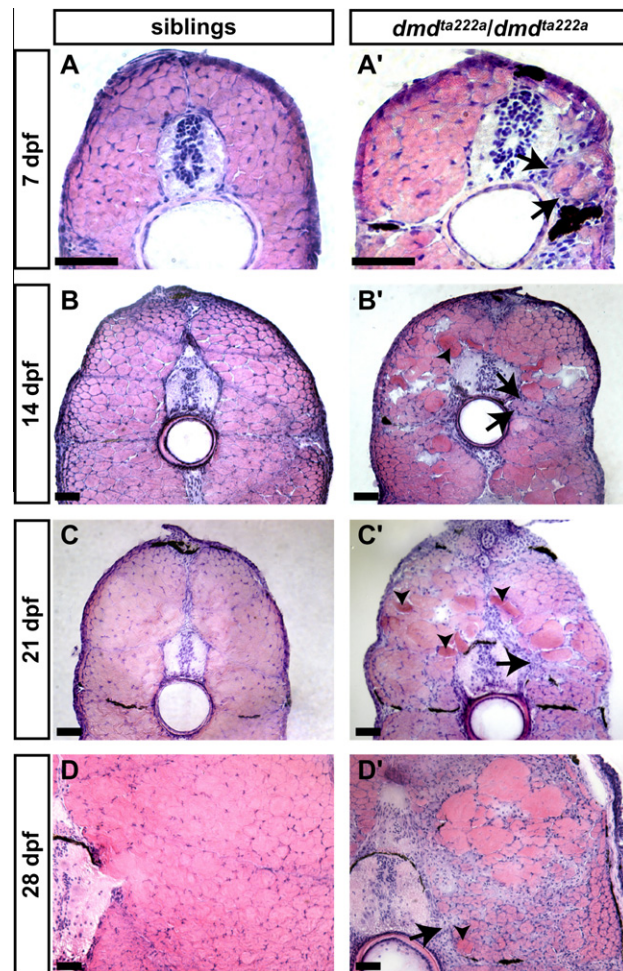


Fig. 2. Progressive pathology of dystrophin-deficient zebrafish. H&E stained cross sections of homozygous *dmd*^{ta222a/ta222a} larvae (A'–D') and their siblings (A–D) at 7 (A and A'), 14 (B and B'), 21 (C and C'), and 28 dpf (D and D'). In comparison to their siblings, the muscle of homozygous *dmd*^{ta222a/ta222a} larvae demonstrates large regions of fibre loss, eosinophilic fibres (indicated by arrowheads in C'), and infiltrates of small mono-nucleated cells (arrows). Scale bar: 50 μ m.

between mammals and fish and the fact that zebrafish predominantly utilise hyperplasia (addition of new fibres) to generate muscle growth, which results in an already high level of central nucleation in the larval myotome. Thus, loss of central nucleation may actually only track the overall fibre loss evident in this animal model.

3.3. Fibrosis and acute inflammatory response of the *dmd*^{ta222a} muscle

The muscle inflammatory response followed by interstitial connective tissue replacement of damaged myofibres is considered a pathological sign of dystrophic muscle. In contrast to their siblings, muscles of 28 dpf old homozygous *dmd*^{ta222a/ta222a} larvae show numerous neutrophils identified by their characteristic electron-dense lamellated granules and eccentric nuclei (Fig. 4A–A') [20]. Neutrophils were also found in clusters, a sign of acute inflammation. In addition, cells with lysosomes and extensive Golgi apparatus, resembling macrophages, were also documented (Supplementary material Fig. S2). Fibrosis was analysed using cross sections of 28 dpf old larvae stained with Azan–Mallory, which stains collagen fibres blue. In comparison to their siblings, *dmd*^{ta222a/ta222a} homozygotes displayed additional interstitial fibrosis between skeletal muscle fibres (Fig. 4B–B').

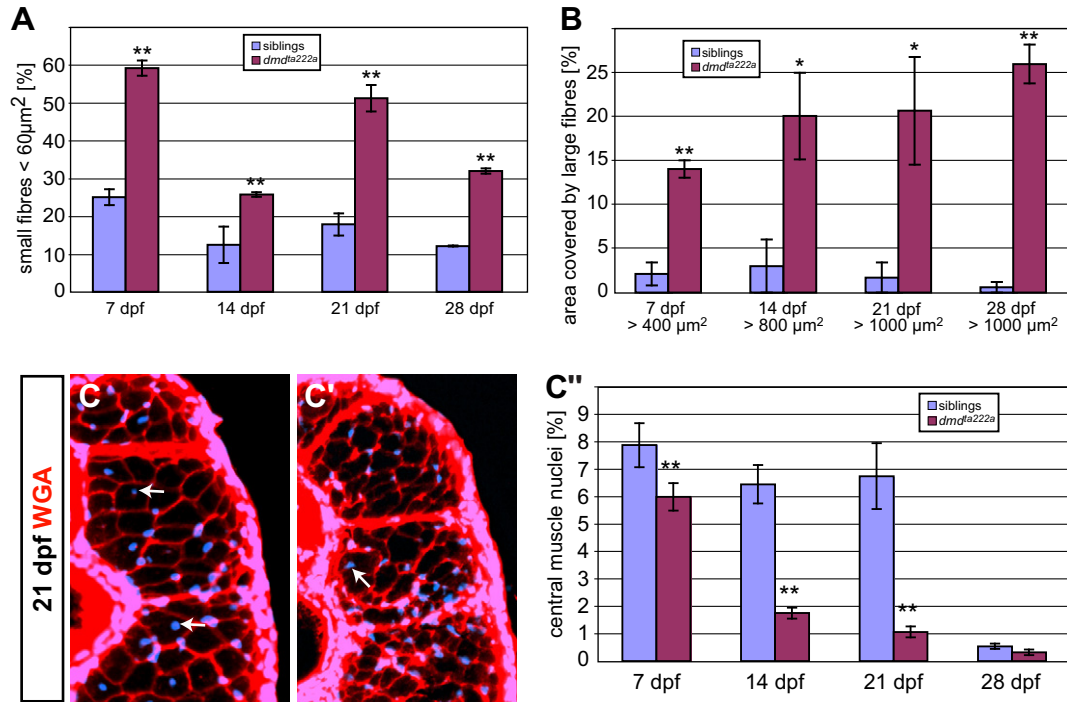


Fig. 3. Dystrophin-deficient zebrafish display a large variation in myofibres CSA. In comparison to their siblings, homozygous *dmd^{ta222a/ta222a}* larvae at 7, 14, 21, and 28 dpf have significantly more myofibres with a CSA below $60 \mu m^2$ ($P < 0.01$, $n = 4$ per stage) (A). Likewise, the area covered by myofibres larger than $400 \mu m^2$ at 7 dpf, $800 \mu m^2$ at 14 dpf, and $1000 \mu m^2$ at 21 and 28 dpf is greater in homozygous *dmd^{ta222a/ta222a}* larvae than in their siblings ($P < 0.01$ for 7 and 28 dpf, $P < 0.02$ for 14 and 21 dpf; $n = 4$ per stage) (B). A reduction of the percentage of myofibres with centralised nuclei is observed in homozygous *dmd^{ta222a/ta222a}* larvae (C') compared to their siblings (C). This reduction is highly significant at 7, 14, and 21 dpf ($P < 0.002$, $n = 5$ for 7 dpf and $n = 4$ for 14, 21, and 28 dpf) (C'). * $P < 0.02$, ** $P < 0.01$ versus siblings. Data are mean \pm SEM.

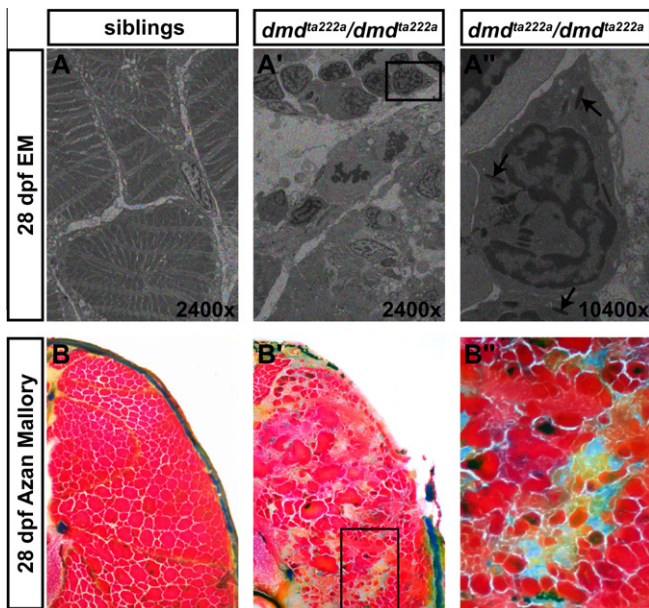


Fig. 4. Inflammation and fibrosis in dystrophin-deficient zebrafish. Neutrophils, identified by their electron dense granules (indicated by arrows), were not detected in the muscle of siblings (A) while in the *dmd^{ta222a/ta222a}* homozygous muscle neutrophils were frequently found (A'), some even clustered, indicative of an acute inflammatory response ($n = 4$ with 4 sections each per larvae). Higher magnification of box in A' (A''). Cross sections stained with Azan–Mallory depict fibrous tissue in blue in homozygous *dmd^{ta222a/ta222a}* muscle (B'), while the sibling's muscle remains largely unstained (B). Higher magnification of box in B' (B'').

3.4. Muscle proliferation of *dmd^{ta222a}* larvae

Loss of dystrophin protein in humans is characterised by cycles of regeneration and degeneration, which is theorised to lead to

premature senescence of muscle stem cells [21,22]. In order to survey the muscle regeneration in *dmd^{ta222a}* zebrafish, cross sections from similar anterior–posterior levels of 7, 14, 21, and 28 dpf old homozygous *dmd^{ta222a/ta222a}* larvae and their siblings were compared. For the 7 dpf stage, 7 pairs of larvae from independent clutches were analysed ($n = 7$), while for each other stage, 4 pairs were used ($n = 4$).

Firstly, proliferation in the muscle was determined via a 60-min pulse of 5-Bromo-2-deoxyuridine (BrdU), which labels S-phase nuclei. Measuring of the BrdU labelling index revealed a highly significant increase in proliferation in the trunk muscle of *dmd^{ta222a/ta222a}* homozygotes compared to their siblings throughout larvae development (Fig. 5A–A'). The increase in proliferation was 5.9 ± 0.3 , 3.7 ± 0.3 , 2.7 ± 0.6 , and 3.4 ± 0.3 -fold for the stages 7, 14, 21, and 28 dpf, respectively (data are means \pm SEM).

Recently we have determined the existence of a Pax7-positive progenitor pool evident in larval skeletal muscle of zebrafish that is similar to satellite cells of amniotes [23,24]. In order to determine if proliferation of the satellite cell pool contributes to the regenerative response in this dystrophin-deficient zebrafish model, cross sections selected as described above were immunostained with antibody against Pax7. Measuring the amount of Pax7-positive cells per 100 myofibre, detected by Phalloidin that stains the actin within a muscle fibre, revealed that throughout larval development homozygous *dmd^{ta222a/ta222a}* larvae have a significantly higher proliferation of the satellite cell population as compared to their siblings (Fig. 5B–B'). The increase in proliferation was 6.1 ± 0.7 , 2.9 ± 0.4 , 2.1 ± 0.2 , and 2.4 ± 0.4 -fold for the stages 7, 14, 21, and 28 dpf, respectively (data in means \pm SEM). The analysis of the BrdU incorporation and the amount of Pax7-positive cells indicate a significantly higher rate of proliferation in the trunk muscle of homozygous *dmd^{ta222a/ta222a}* larvae in comparison to their siblings, similar to the human DMD condition.

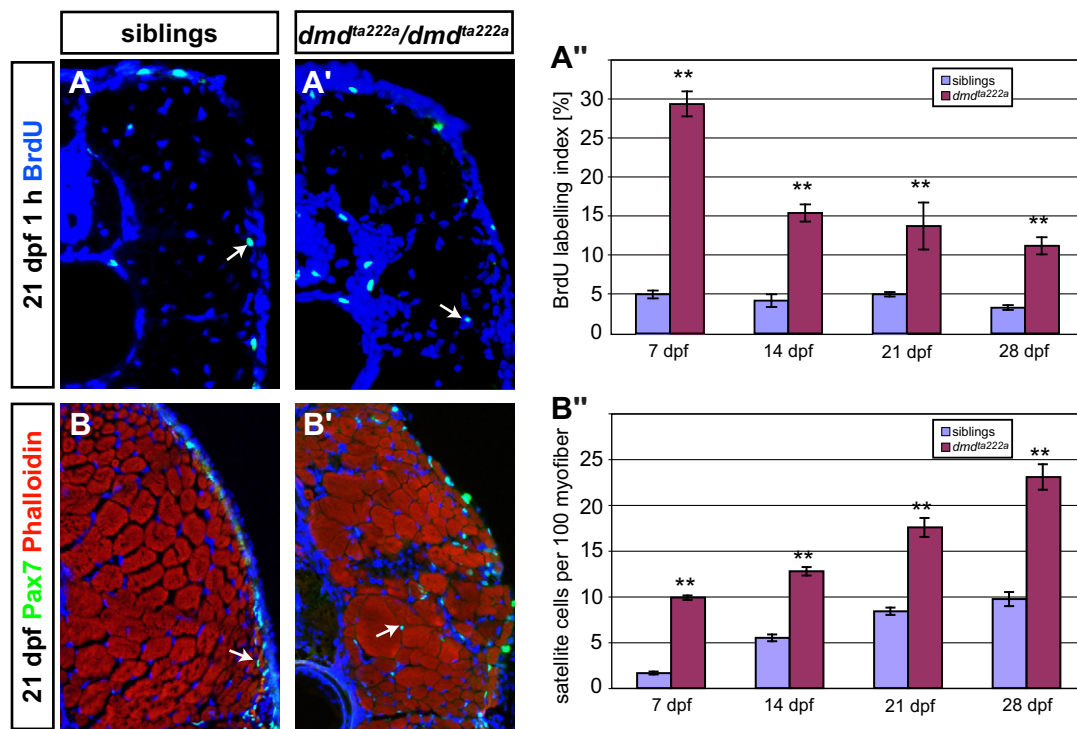


Fig. 5. Muscle proliferation in dystrophin-deficient zebrafish. After a 1 h pulse of BrdU, cross sections of siblings (A) and homozygous *dmd*^{ta222a/ta222a} larvae (A') at 21 dpf were immunostained for BrdU (green) and Hoechst (blue) and the BrdU labelling index was measured. At 7, 14, 21, and 28 dpf homozygous *dmd*^{ta222a/ta222a} muscle show a highly significant increase in the BrdU labelling index ($P < 0.0001$, $n = 7$ for 7 dpf and $n = 4$ for 14, 21, and 28 dpf) (A''). Cross sections of 21 dpf old homozygous *dmd*^{ta222a/ta222a} larvae (B') and their siblings (B) were immunostained for Hoechst (blue), Pax7 (green) and Phalloidin (red). Comparison of the amount of Pax7-positive cells per 100 myofiber in homozygous *dmd*^{ta222a/ta222a} larvae and their siblings shows a highly significant increase in Pax7 cells in *dmd*^{ta222a/ta222a} homozygotes ($P < 0.01$, $n = 4$ per larvae stage) (B''). ** indicates $P < 0.01$. Data are mean \pm SEM.

3.5. Detaching fibres

To directly analyse muscle pathology of dystrophin-deficient zebrafish *in vivo*, we used time-lapse photomicroscopy. Anaesthetised 3 dpf old *dmd*^{ta222a/ta222a} larvae were mounted in agarose ($n = 8$). During the period in which larvae remain anaesthetised no myofibre loss could be observed. Upon withdrawal of the anaesthetic, however, the muscle of the mutant larvae began to contract and individual fibres were observed detaching from their myotendinous junction and retracting back into the myotome (Fig. 6 and Supplementary movie S1). Each detachment event typically lasted 10 s from the beginning of detachment to full retraction. These events only occurred upon withdrawal of the anaesthetic indicating that myofibre detachment was dependant upon mechanical load applied by the onset of strong muscle contraction. Siblings from the same clutch did not exhibit fibre detachment under identical conditions ($n = 8$).

4. Discussion

This report describes that the dystrophin-deficient zebrafish mutant *dmd* resembles many aspects of the human DMD condi-

tion. Furthermore we suggest that the zebrafish as a model system offers specific advantages such as genetic manipulability, optical clarity of the embryo and larvae, and efficient husbandry, suggesting that the zebrafish *dmd* mutant could be a highly valuable paradigm in which to study the pathological consequence of the loss of dystrophin *in vivo*.

As in human [14,15], the expression of zebrafish dystrophin in myofibres gradually shifts from a junctional myotendinous location in the embryo to the non-junctional sarcolemma at later stages, failure of which is believed to be the major cause of the human pathology. The progressive increase in expression of dystrophin protein at non-junctional sites in zebrafish correlates well with a number of pathological similarities between the dystrophin-deficient zebrafish and the human condition. The hallmark of the human DMD pathology is marked myofibre loss followed by muscle regeneration, which was also detected in *dmd*^{ta222a} mutants throughout the larvae stages from 7 to 28 dpf. Connective tissue accumulation at the site of muscle loss is the other major characteristic of DMD pathology and is considered to be secondary to the degeneration of muscle tissue. The phenomenon may be viewed as a pivotal event in the dystrophic process since it leads to a seemingly irreversible loss of muscle tissue organization and

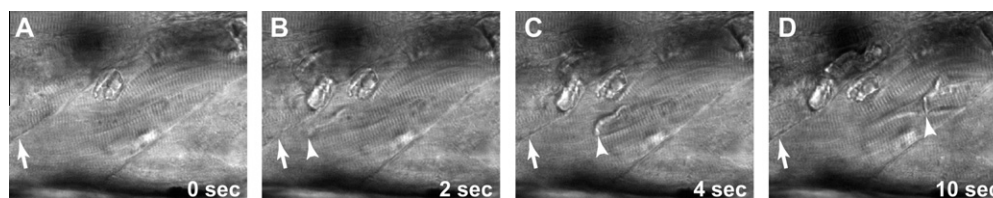


Fig. 6. Detaching myofibre monitored by time-lapse microscopy. Removal of the anaesthetic provokes muscle contraction in a 3 dpf old homozygous *dmd*^{ta222a/ta222a} larvae encased in agarose. A myofibre that is attached to the myotendinous junction (arrow in A) at the beginning of the time-lapse movie detaches and, over the time course of 10 s, the end of the myofibre (arrowhead) retracts into the somite (B–D) leaving an evident retraction groove.

permanent replacement of muscle fibres with fat and connective tissue [25]. In homozygous *dmd^{ta222a/ta222a}* larvae deposits of collagen were documented by Azan–Mallory staining. In addition, the proliferation of cells located inside the muscle tissue, as documented by calculation of the BrdU labelling index, is significantly enhanced. After 7 dpf the proliferation rate of the BrdU-positive cells was more enhanced than the proliferation of the muscle specific, Pax7-positive satellite cells, which might point to a proliferation of fibroblasts at the site of muscle injury. Furthermore, this fibrosis is accompanied by infiltration of neutrophils, a similar process as monitored in DMD patients. Interestingly, the detected enhanced proliferation of muscle satellite cells in *dmd^{ta222a}* mutants is not able to generate sufficient myofibres to compensate for fibre loss, as large gaps and areas of mono-nucleated cellular infiltrates were documented inside the muscle of *dmd^{ta222a/ta222a}* homozygotes. The muscle of DMD patients displays a marked variation in the size of myofibres that can range from the smallest fibres barely visible to some documented hypertrophic fibres being as large as 50,000 μm^2 [19], a tendency paralleled in the zebrafish *dmd^{ta222a}* mutant. As in human DMD patients, some hypertrophic fibres were extremely large (up to 9000 μm^2) in comparison to an average fibre size, depending on the larvae stage, of 130–220 μm^2 in siblings. Furthermore, the detection of scattered eosinophilic fibres in the muscle of *dmd^{ta222a}* mutants reflects the muscle pathology of affected human embryos [18]. While the majority of analyses revealed phenotypic concordance between the pathology of mammalian and piscine dystrophic tissue, one parameter showed a distinct response. The level of centralised nuclei evident in muscle syncytia was significantly decreased in *dmd^{ta222a}* mutants, the reverse of the mammalian dystrophic pathology. This may reflect a difference between the way that fish and mammalian muscle growth proceeds. While post-natal growth of mammalian muscle occurs almost exclusively via hypertrophy, fish muscle is generated both by hyperplastic and hypertrophic growth in the larval phase [26]. Hence, central nucleation is at a high level normally in zebrafish muscle. These centrally nucleated “intermediate” fibres may be preferentially lost during the dystrophic response, while more mature fibres may actually undergo the massive hypertrophic growth evident via the presence of some extraordinarily large diameter fibres in dystrophic zebrafish. In addition, nuclei of regenerating mouse myofibres exhibit a peripheral relocalisation that is faster in neonatal than in adult mice suggesting that even within mammals central nucleation may not be the most reliable measure of fibre age [27]. Furthermore, newborn muscle fibres in zebrafish are much smaller than their mammalian counterparts and very difficult to score for nuclei positioning, as the nucleus makes up a large percentage of the diameter of newborn fibres. Therefore, analysis of the central nucleation is not an appropriate parameter to measure regeneration in the zebrafish. Nevertheless, the significant increase in both proliferation and the number of small myofibres within the zebrafish *dmd^{ta222a}* mutant resembles muscle regeneration evident in human DMD patients.

In addition, the role of dystrophin as a mechanical link between the extracellular matrix and the cytoskeleton for fibre detachment was studied. For this purpose, we made use of the dystrophin-deficient zebrafish model being translucent and studied for the first time myofibre detachment by live imaging *in vivo* in a dystrophin loss-of-function context. Interestingly, detaching myofibres could only be observed in larvae recovered from their anaesthesia and undergoing active muscle contraction, indicating that muscle load is an important component of triggering the loss of dystrophin-deficient myofibres. This data supports the hypothesis that dystrophin at least partially functions as a mechanical link between the extracellular matrix and the myofibre cytoskeleton.

Taken together, the phenotype and pathology of homozygous *dmd^{ta222a/ta222a}* larvae resembles most aspects of human DMD, pro-

viding a genetically amenable model in which dystrophin loss can be surveyed. Obtained data suggest that due to the advantages of the zebrafish as an animal model system novel experiments, as prospective high-throughput small molecule screens [11], could be performed to gain novel insights into DMD in humans.

Acknowledgements

We are grateful to M.D. Grounds (University of Western Australia, Australia) for comments on the manuscript. P.D.C. was supported by the National Health and Medical Research Council of Australia.

Appendix A. Supplementary data

Supplementary data associated with this article can be found, in the online version, at doi:10.1016/j.nmd.2010.08.004.

References

- [1] Ervasti JM, Sonnemann KJ. Biology of the striated muscle dystrophin-glycoprotein complex. *Int Rev Cytol* 2008;265:191–225.
- [2] Allen DG, Gervasio OL, Yeung EW, Whitehead NP. Calcium and the damage pathways in muscular dystrophy. *Can J Physiol Pharmacol* 2010;88:83–91.
- [3] Bulfield G, Siller WG, Wight PA, Moore KJ. X Chromosome-linked muscular dystrophy (mdx) in the mouse. *Proc Natl Acad Sci USA* 1984;81:1189–92.
- [4] Hoffman EP, Brown Jr RH, Kunkel LM. Dystrophin: the protein product of the duchenne muscular dystrophy locus. *Cell* 1987;51:919–28.
- [5] Dubowitz V. Therapeutic efforts in duchenne muscular dystrophy; the need for a common language between basic scientists and clinicians. *Neuromuscul Disord* 2004;14:451–5.
- [6] Zucconi E, Valadares MC, Vieira NM, et al. Ringo: discordance between the molecular and clinical manifestation in a golden retriever muscular dystrophy dog. *Neuromuscul Disord* 2009.
- [7] Lieschke GJ, Currie PD. Animal models of human disease: zebrafish swim into view. *Nat Rev* 2007;8:353–67.
- [8] Granato M, van Eeden FJ, Schach U, et al. Genes controlling and mediating locomotion behavior of the zebrafish embryo and larva. *Development* 1996;123:399–413.
- [9] Bassett DI, Bryson-Richardson RJ, Daggett DF, Gautier P, Keenan DG, Currie PD. Dystrophin is required for the formation of stable muscle attachments in the zebrafish embryo. *Development* 2003;130:5851–60.
- [10] Bassett D, Currie PD. Identification of a zebrafish model of muscular dystrophy. *Clin Exp Pharmacol Physiol* 2004;31:537–40.
- [11] Berger J, Currie P. The role of zebrafish in chemical genetics. *Curr Med Chem* 2007;14:2413–20.
- [12] Berger J, Berger S, Tuoc TC, et al. Conditional activation of pax6 in the developing cortex of transgenic mice causes progenitor apoptosis. *Development* 2007;134:1311–22.
- [13] Pena SD, Gordon BB, Karpatis G, Carpenter S. Lectin histochemistry of human skeletal muscle. *J Histochem Cytochem* 1981;29:542–6.
- [14] Wessels A, Ginjaar IB, Moorman AF, van Ommen GJ. Different localization of dystrophin in developing and adult human skeletal muscle. *Muscle Nerve* 1991;14:1–7.
- [15] Clerk A, Strong PN, Sewry CA. Characterisation of dystrophin during development of human skeletal muscle. *Development* 1992;114:395–402.
- [16] Bolanos-Jimenez F, Bordais A, Behra M, Strahle U, Sahel J, Rendon A. Dystrophin and dp71, two products of the *dmd* gene, show a different pattern of expression during embryonic development in zebrafish. *Mech Dev* 2001;102:239–41.
- [17] Chambers SP, Dodd A, Overall R, et al. Dystrophin in adult zebrafish muscle. *Biochem Biophys Res Commun* 2001;286:478–83.
- [18] Emery AE, Burt D. Intracellular calcium and pathogenesis and antenatal diagnosis of duchenne muscular dystrophy. *Br Med J* 1980;280:355–7.
- [19] Dubowitz V, Sewry CA. Muscle biopsy – a practical approach. 3rd ed. East Sussex United Kingdom: Saunders Elsevier; 2007.
- [20] Lieschke GJ, Oates AC, Crowhurst MO, Ward AC, Layton JE. Morphologic and functional characterization of granulocytes and macrophages in embryonic and adult zebrafish. *Blood* 2001;98:3087–96.
- [21] Decary S, Hamida CB, Mouly V, Barbet JP, Hentati F, Butler-Browne GS. Shorter telomeres in dystrophic muscle consistent with extensive regeneration in young children. *Neuromuscul Disord* 2000;10:113–20.
- [22] Webster C, Blau HM. Accelerated age-related decline in replicative life-span of duchenne muscular dystrophy myoblasts: implications for cell and gene therapy. *Somatic Cell Mol Genet* 1990;16:557–65.
- [23] Hollway GE, Bryson-Richardson RJ, Berger S, Cole NJ, Hall TE, Currie PD. Whole-somite rotation generates muscle progenitor cell compartments in the developing zebrafish embryo. *Dev Cell* 2007;12:207–19.
- [24] Relaix F, Rocancourt D, Mansouri A, Buckingham M. A pax3/pax7-dependent population of skeletal muscle progenitor cells. *Nature* 2005;435:948–53.

- [25] Duance VC, Stephens HR, Dunn M, Bailey AJ, Dubowitz V. A role for collagen in the pathogenesis of muscular dystrophy? *Nature* 1980;284:470–2.
- [26] Patterson SE, Mook LB, Devoto SH. Growth in the larval zebrafish pectoral fin and trunk musculature. *Dev Dyn* 2008;237:307–15.
- [27] Grounds M, Partridge TA, Sloper JC. The contribution of exogenous cells to regenerating skeletal muscle: an isoenzyme study of muscle allografts in mice. *J Pathol* 1980;132:325–41.